Supporting Information

Programmed Nanococktail Based on pH-Responsive Function Switch for Self-Synergistic Tumor-Targeting Therapy

Yang Li, [1*] Liang Song, [1] Jinyan Lin, [1, 3] Jinyuan Ma, [2] Zhou Pan, [1] Yinying Zhang, [1] Guanghao Su, [5] Shefang Ye, [1] Fang-hong Luo, [4] Xuan Zhu, [2] Zhenqing Hou [1*]

[1] Department of Biomaterials, College of Materials, Xiamen University, Xiamen 361005, China.

[2] School of Pharmaceutical Science, Xiamen University, Fujian Provincial Key Laboratory of Innovative Drug Target Research, Xiamen 361005, P. R. China

[3] The State Key Laboratory of Physical Chemistry of Solid Surface, Department of Chemistry, College of Chemistry & Chemical Engineering, Xiamen University, Xiamen 361005, China

[4] Cancer Research Center, Medical College, Xiamen University, Xiamen 361005, P. R. China

[5] Children's Hospital of Soochow University, Suzhou 215025, P. R. China

*Corresponding author: Yang Li, E-mail address: liyang@xmu.edu.cn

*Corresponding author: Zhenqing Hou, E-mail address: houzhenqing@xmu.edu.cn

ORCID

Yang Li: 0000-0001-8950-1212

Zhenqing Hou: 0000-0002-5537-075X

1. Supplementary Methods and Measurements

1.1 Materials. All chemical reagents were of analytical grade and used without further purification unless otherwise stated. Deionized (DI) water was used throughout. Epirubicin (EPI, purify ≥ 99.9%) was purchased from Zhejiang Hisun Pharmaceutical Co., Ltd. (China). Phospholipid (PC, e.g. soybean lecithin) was provided by Lipoid GmbH (Ludwigshafen, Germany). 1, 2-distearoyl-sn-glycero-3-phosphoethanolamine (DSPE), 1, 2-distearoyl-sn-glycero-3-phosphoethanolamine-N-[carboxyl(polyethylene glycol)-2000] (DSPE-PEG-COOH) and 1, 2-distearoyl-sn-glycero-3-phosphoethanolamine-N-[methoxy(polyethylene glycol)-2000] (DSPE-MPEG) were provided by Avanti Polar Lipids. Bis-hydroxyl poly(ethyleneglycol) (PEG, molecular weight of ~2000) was provided Sinopeg Biotech Co., Ltd. (Xiamen, China). Methotrexate (MTX, purify ≥ 98.0%) and folic acid (FA, purify ≥ 96.0%) were purchased from Bio Basic Inc. (Markham, Ontario, Canada). N, N'-dicyclohexylcarbodiimide (DCC), N-hydroxysuccinimide (NHS), and N, N'-disuccinimidyl carbonate (DSC) were purchased from Sigma-Aldrich Co., Ltd. (St. Louis, MO, USA). 1'-dioctadecyl-3, 3, 3', 3'-tetramethylindotricarbocyanine iodide (DiR), 1, 1'-dioctadecyl-3, 3, 3', 3'-tetramethylindodicarbocyanine perchlorate (DiD), and 4', 6-diamidino-2-phenylindole dihydrochloride (DAPI) were obtained from Molecular Probes Inc. (Eugene, OR, USA). 3-(4, 5-dimethylthiazol-2-yl)-2, 5-diphenyltetrazolium bromide (MTT) was purchased from Amresco (Solon, OH, USA). Dulbecco's modified Eagle's medium (DMEM) and 0.25% trypsin were purchased from M&C Gene Technology (Beijing, China). Penicillin-streptomycin and trypsin-ethylenediamine tetra-acetic acid (EDTA) were Hyclone (USA). Fetal bovine serum (FBS) was purchased from Gibco Life Technologies (AG, Switzerland).

1.2 Synthesis of DSPE-PEG-CH=N-MTX. Firstly, DSPE-PEG-hydroxyl (DSPE-PEG-OH) was synthesized according to the reported literature. [1] Secondly, DSPE-PEG-aldehyde (DSPE-PEG-CHO) was synthesized by the oxidation of DSPE-PEG-OH with acetic anhydride in dimethyl sulfoxide (DMSO)/chloroform according to the reported procedure. [2] Finally, DSPE-PEG-CH=N-MTX was synthesized starting from DSPE-PEG-CHO and MTX molecule through reductive amination via Schiff's base formation. DSPE-PEG-CHO (56.2 mg, 20 μmol) and MTX (13.6 mg, 30 μmoL) were dissolved in 20 mL of DMSO/chloroform in a round-bottom flask, and then a few drops of acetic acid were dropped into the flask

with molecular sieves. The mixture was degassed through three freeze-pump-thaw procedure and reacted at 40ºC for 48 h. The resultant product was evaporated and precipitated into excess dry, ice-cold ethyl ether and acetone (10:1) mixture. The crude precipitate was separated by decantation and redissolved in dichloromethane (DCM). The unreacted or excess MTX was removed from the conjugated one via filtration. The filtrate was concentrated and reprecipitated into a mixture of ice-cold ethyl ether and acetone (10:1). The reprecipitate was separated by decantation, washed thrice with ice-cold ethyl ether to remove traces of DMSO, dried in vacuum overnight, and stored at -20 ºC.

In addition, DSPE-PEG-MTX was synthesized starting from DSPE-PEG-COOH and MTX molecule via amide bond according to our previous works with some modification. [3-6] In a typical reaction, DSPE-PEG-COOH (84.8 mg, 30 μmol), DCC (7.5 mg, 36 μmol) and NHS (4.2 mg, 36 μmol) were dissolved in DMSO with continuous stirring under a nitrogen atmosphere. After 30 min, MTX (20.4 mg, 45 μmoL) was added to a DMSO solution containing the activated DSPE-PEG-COOH. The mixture was allowed to react at 30 ºC for 72 h with continuous stirring under a nitrogen atmosphere. The resulting mixture was filtered to remove the white precipitation of dicylcohexyl urea (DCU) and precipitated in an ice-cold mixture of ethyl ether and acetone (10:1). The crude precipitate was separated by decantation and redissolved in DCM. The unreacted or excess MTX was removed from the conjugated one via filtration. The filtrate was concentrated and reprecipitated into a mixture of ice-cold ethyl ether and acetone (10:1). The reprecipitate was separated by decantation, washed thrice with ice-cold ethyl ether to remove traces of DMSO, dried in vacuum overnight, and stored at -20 ºC.

1.3 Characterization of DSPE-PEG-CH=N-MTX. The ^{1}H nuclear magnetic resonance (NMR) spectrum was determined on a Bruker AV400 MHz NMR spectrometer (Bruker, Billerica, MA, USA). The ultraviolet-visible (UV-vis) absorption spectrum was recorded with a Perkin Elmer Lambda 750 UV-vis-near-infrared spectrophotometer (Perkin-Elmer, Norwalk CT). The matrix-assisted laser desorption/ionization time-of-flight mass (MALDI-TOF-MS) spectrum was acquired by a Bruker Reflex III MALDI-TOF mass spectrometer (Bruker Daltonics, Bremen, Germany). The molecular weight was determined by gel permeation chromatography using Waters analytical columns Styragel HT2 (7.8 × 300 mm). Tetrahydrofuran (THF) was used as the mobile phase at a flow rate of 1.0

ml/min under 30 ºC.

1.4 Fabrication of EPI-PC Complex. The EPI-PC was synthesized by a co-solvent technique based on our previous reported study with some modications. [7] Firstly, 10 mg of EPI and 25 mg of PC were added into 12 mL of THF and continuously stirred at 45 ℃. The resulting mixture became clear and transparent in 24 h, indicating the dispersion of EPI-PC complex was formed. Subsequently, the organic solvent was removed through vacuum rotary evaporation, obtaining the film of the crude EPI-PC complex.

In order to determine the complexation rate of EPI and PC in the formation of EPI-PC complex, the crude EPI-PC complex was added into DCM (insoluble solvent of EPI), followed by the vigorous vortexing, and filtered through a 220 nm pore-size membrane filter to remove the excess and uncomplexed EPI. The filtrate was evaporated to dryness and the purfied EPI-PC complex was subjected to high performance liquid chromatography (HPLC, Shimadzu, CBM-20A) analysis. The complexation rate of EPI-PC complex was calculated by the following eqn (1).

$$\text{Complexation rate}(\%) = \frac{\text{W(complexed)}}{\text{W(total)}} \times 100\% \quad (1)$$

where W(complexed) and W(total) means the amount of the complexed EPI and the total amount of EPI added in the fabrication of EPI-PC complex, respectively.

1.5 Characterization of EPI-PC Complex. The ^{1}H-NMR spectrum was performed on a Bruker AVANCE III 400MHz NMR spectrometer (Bruker, Germany). The solvent for EPI and physical mixture of EPI and PC was deuterated dimethyl sulfoxide (DMSO-d_6), and that for PC and EPI-PC complex was deuterated chloroform ($CDCl_3$). The differential scanning calorimetry (DSC) curve was performed by differential scanning calorimeter (DSC 204F1, Netzsch, Selb, Germany). The X-ray diffraction (XRD) spectrum was recorded by an X-ray diffractometer (Phillips X'pert Pro Super, Panalytical, Almelo, Netherlands). The fourier transform infrared (FT-IR) spectrum was performed on a Bruker IFS-55 infrared spectrometer (Bruker, Switzerland). The fluorescence spectrum was recorded with a FluoroMax-4 Spectrofluorometer (HORIBA Jobin Yvon Inc., NY, USA). The morphology was observed by transmission electron microscopy (TEM, JEM 1400, JEOL, Tokyo, Japan). EPI, PC, and physical mixture of EPI and PC were used as controls for comparison

1.6 Preparation of MTX-PEG-EPI-PC NPs. The MTX-PEG-EPI-PC NPs were

prepared by a lipid hydration method followed by an extrusion technique. Briefly, EPI-PC complex (15 mg) and DSPE-PEG-MTX (10 mg) were dissolved in chloroform, and the organic solvent was evaporated by gentle heating under vacuum in the dark. The resultant dried thin lipid film was dispersed in 20 mL of distilled (DI) water via vigorous stirring and ultrasonication. After stirring for 10 min, the MTX-PEG-EPI-PC NPs were sonicated on ice for 30 min with 10 s intervals. After that, the unincorporated drug (precipitate) was removed through polycarbonate membranes with 0.2 and 0.1 μm pores using a Mini-extruder (Avanti, USA) by 10 extrusion cycles. The drug concentration of MTX-PEG-EPI-PC NPs was determined through high performance liquid chromatography (HPLC, Shimadzu, CBM-20A) method as described in the literature. [8-9]

The PEG-EPI-PC NPs were prepared using the identical procedure except that DSPE-PEG-CH=N-MTX was replaced by DSPE-MPEG at the equivalent molar for addressing the specificity of MTX-PEG-EPI-PC NPs towards FA receptors. The MTX-PEG-EPI-PC NPs (via amide bond) were prepared using the identical procedure except that DSPE-PEG-CH=N-MTX was replaced by DSPE-PEG-MTX (conjugated between carboxyl group DSPE-PEG-COOH and aromatic amino group of MTX) at the equivalent molar for addressing the target release of MTX-PEG-EPI-PC NPs (via imine bond) towards acidic endo/lysosomes.

1.7 Preparation of Probe-Loaded MTX-PEG-EPI-PC NPs. In a typical procedure for the preparation of probe-loaded MTX-PEG-EPI-PC NPs: EPI-PC complex (15 mg) and DSPE-PEG-MTX (10 mg) were dissolved in chloroform followed by adding a certain amount of probe (DiD or DiR). Then, the organic solvent was evaporated by gentle heating under vacuum in the dark. The resultant dried thin lipid film was dispersed in 20 mL of distilled (DI) water via vigorous stirring and ultrasonication. After stirring for 10 min, the probe-loaded MTX-PEG-EPI-PC NPs were sonicated on ice for 30 min with 10 s intervals. After that, the unincorporated drug (precipitate) was removed through polycarbonate membranes with 0.2 and 0.1 μm pores using a Mini-extruder (Avanti, USA) by 10 extrusion cycles. The probe-loaded PEG-EPI-PC NPs and MTX-PEG-EPI-PC NPs (via amide bond) were prepared using the identical procedure except that DSPE-PEG-CH=N-MTX was replaced by DSPE-MPEG and DSPE-PEG-MTX at the equivalent molar, respectively.

1.8 Characterization of MTX-PEG-EPI-PC NPs. The hydrodynamic particle size and polydispersity index (PDI) was determined by dynamic light scattering (DLS)

using a Malvern Zetasizer 2000 (Malvern Instruments, Worcestershire, U.K.). The zeta potential was determined by electrophoretic light scattering (ELS) using a same equipment. The morphology was visualized through scanning electron microscopy (SEM, LEO1530VP, Carl Zeiss AG, Germany) operated at an accelerating voltage of 20 kV, transmission electron microscopy (TEM, JEM2100, JEOL, Japan) operated at an accelerating voltage of 200 kV, and atomic force microscopy (AFM, Multimode 8, Bruker USA) operated in tapping mode. The fluorescence dye labeled NPs were observed using a Leica TCS SP5 confocal laser scanning microscopy (Leica Microsystems, Mannheim, Germany).

1.9 Drug-Loading Content. To measure the amount of EPI or MTX loaded (encapsulated or conjugated) within MTX-PEG-EPI-PC NPs, the lyophilized MTX-PEG-EPI-PC NPs were dissolved in anhydrous DMSO by ultrasonication. After the filtration by 0.22 μm filter membrane, a part of the filtrate was analyzed for the determination of drug loading content by a high-performance liquid chromatography (HPLC) method as described above. The drug loading content of MTX-PEG-EPI-PC NPs was calculated as (Amount of drug in MTX-PEG-EPI-PC NPs)/ (Weight of MTX-PEG-EPI-PC NPs) × 100%.

1.10 *In Vitro* Stability. The *in vitro* stability of MTX-PEG-EPI-PC NPs was performed under different media by incubating MTX-PEG-EPI-PC NPs in DI water, phosphate buffer saline (PBS) solution, cell culture medium (DMEM), and DMEM with 10% FBS for 60 h. At specific time intervals, the hydrodynamic particle size, PDI, and zeta potential of MTX-PEG-EPI-PC NPs was determined by DLS.

1.11 *In Vitro* Drug Release. The drug release profile of EPI (or MTX) from MTX-PEG-EPI-PC NPs was evaluated in buffer solution at 37 ℃. 1 mL of MTX-PEG-EPI-PC NPs was transferred into a dialysis membrane (molecular weight cut-off of 1000 Da) and then immersed into 49 mL of buffer solution. The medium was kept at 37 ℃ with gentle shaking. At the selected time intervals, 1 mL of the release medium was withdrawn and the release medium was replaced with an equal volume of fresh medium. The released EPI or MTX at different time points was analyzed by fluorescence method and high-performance liquid chromatography (HPLC) method, respectively. The conditions of HPLC method were as follows: stationary phase, Hypersil ODS column (250 mm × 4.6 mm, 5 μm); temperature, 25 ℃; elution flow rate, 1.0 mL/min; detection wavelength, 303 nm; mobile phase, HPLC grade acetonitrile/0.04 M potassium dihydrogen phosphate (pH 4.5) (12/88,

v/v). [9] The accumulative drug release of MTX-PEG-EPI-PC NPs was expressed as a percentage of the released drug. The drug release profile of the free drug (EPI and MTX) and PEG-EPI-PC NPs was used as controls for comparison. The cumulative release amount was calculated using eqn (2).

$$\text{Cumulative release}\,(\%) = \frac{1\times \sum_{i=1}^{n-1} \text{Ci} + 50\times \text{Cn}}{\text{weight of drug in nanosystems}} \times 100\% \quad (2)$$

where *Ci* means the concentration of EPI or MTX drug in dialysate at *i* time.

1.12 Cell Culture. HeLa human cervical carcinoma cells, MCF-7 human breast carcinoma cells, A549 human lung carcinoma cells, and NIH-3T3 mouse fibroblastic cells were cultured in FA-deficient DMEM (DMEM without FA). All the cell lines were was obtained from American Type Culture Collection (ATCC) and grew at the culture media supplemented with 10% fetal bovine serum (FBS) and 1% antibiotics (100 U/mL penicillin and 100 U/mL streptomycin). The cells were cultured in an incubator (Thermo Scientific) at 37 ºC under a humidified atmosphere containing 5% CO_2.

1.13 *In Vitro* Cellular Uptake. For quantitative study, confocal imaging of cells was performed using a Leica laser scanning confocal microscope (Leica Microsystems, Mannheim, Germany). Confocal imaging of EPI was performed using a laser with a peak wavelength of 488 nm as the excitation source. HeLa cells were cultured in 6-well plates with at a density of 1×10^5 cells per well. The cells were incubated at 37 °C and 5% CO_2 for 24 h. 100 μL of MTX-PEG-EPI-PC NPs (EPI: 2 μg/mL) in the absence or presence of free FA were added to the cells for specific incubation periods (1, 4, and 8 h). After incubation, the cells were washed with PBS, fixed with 4% paraformaldehyde, stained with DAPI and imaged using a Leica TCS SP5 confocal laser scanning microscope (CLSM, Leica Microsystems, Germany). The cells incubated with PEG-EPI-PC NPs at the equivalent EPI concentration in the absence or presence of free FA were used as controls for comparison.

1.14 Flow Cytometry Analysis. HeLa cells were seeded in 6-well plates with a density of 1×10^5 cells/mL and incubated for 24 h, and then incubated with MTX-PEG-EPI-PC NPs (EPI: 2 μg/mL) in the absence or presence of free FA for specific incubation periods. After harvesting with trypsin-EDTA, the cells were washed with PBS, and the fluorescence was measured using flow cytometry (FACSCalibur, BD Biosciences, USA) with excitation wavelengths of 488 nm. The

cells incubated with PEG-EPI-PC NPs at the equivalent EPI concentration in the absence or presence of free FA were used as controls for comparison.

1.15 Subcellular Location. HeLa cells were seeded into 24-well plate at a density of 1.0×10^4 cells per well. After culture for 24 h, the cells were treated with MTX-PEG-EPI-PC NPs at 37 °C for predetermined incubation time periods. Subsequently, the cells were stained by 200 nM of Lysotracker Green DND-26 (Gibco Life Technologies, AG, Switzerland) at 37 °C for 20 min and fixed with 4% paraformaldehyde for 15 min. Finally, the cells were washed by cold PBS twice, stained with DAPI for 10 min, and observed using a Leica TCS SP5 confocal laser scanning microscopy. The free EPI and PEG-EPI-PC NPs were used as controls.

1.16 Intracellular Both Drugs Co-Delivery. To investigate the intracellular dual-drug delivery of both EPI and MTX from MTX-PEG-EPI-PC NPs, NBD-NH_2 labeled DSPE-PEG-CH=N-MTX was synthesized (DSPE-PEG-CH=N-MTX-NBD was coupled between DSPE-PEG-CH=N-MTX and NBD-NH_2 via amide linkage, **Figure S5**) for use as a fluorescent probe. HeLa cells were seeded, cultured for 24 h at 37 °C and 5% CO_2, and then incubated with NBD-MTX-PEG-EPI-PC NPs for 1 and 12 h. After incubation, the cells were washed with PBS for three times, fixed with 4% (v/v) paraformaldehyde for 15 min, and imaged using a Leica TCS SP5 confocal laser scanning microscopy.

1.17 *In Vitro* Cytotoxicity. The *in vitro* cytotoxicity of MTX-PEG-EPI-PC NPs was measured using a 3-(4, 5-dimethylthiazol-2-yl)-2, 5-diphenyltetrazolium bromide (MTT) assay according to the manufacturer's suggested procedures. HeLa or MCF-7 cells (highly expressed folate receptors) were treated with MTX-PEG-EPI-PC NPs at the equivalent EPI (0.2, 1, 5, 10, and 20 μg/mL) or MTX concentrations (0.083, 0.42, 2.1, 4.2, and 8.4 μg/mL) for 24 h at 37 °C and 5% CO_2. The data were expressed as the percentage of surviving cells. The cells incubated with free EPI, free EPI plus free MTX, and PEG-EPI-PC NPs at the equivalent EPI or MTX concentration were used as controls for comparison. Cell viability (%) was calculated as (OD of test group)/ (OD of control group) × 100%, in which OD was optical density.

In addition, the combination index CI_X was calculated as (IC_X of EPI in the MTX-PEG-EPI-PC NPs)/ (IC_X of EPI in the free EPI) + (IC_X of MTX in the MTX-PEG-EPI-PC NPs)/ (IC_X of MTX in the free MTX), in which X was 10, 20, 30, 40, 50, 60, 70, 80, and 90, respectively.

1.18 *In Vitro* Apoptosis Assay. Apoptosis of HeLa and MCF-7 cells was detected

using the Annexin V-FITC Apoptosis Detection Kit (BD Biosciences). The cells (1.0 × 10^5 cells per well) were seeded in 6-well plates. After culture for 48 h, the cells were respectively treated with PBS, free EPI, free EPI plus free MTX, PEG-EPI-PC NPs, and MTX-PEG-EPI-PC NPs for 24 h. The subsequent procedures were performed according to the manufacturer's suggested procedures. The cells were analyzed by flow cytometry (FACSCalibur, BD Biosciences, USA) and CellQuest/FlowJo (Tree Star, USA) software.

1.19 Animals. All BALB/c nude mice (female, 5-6 weeks, 16-18 g) were provided by Experimental Animal Laboratory of Cancer Research Center of Xiamen University and kept under specific pathogen-free (SPF) conditions with free access to standard food and water. Before drug administration, all animals were acclimatized for 1 week under 25 ± 2°C and a humidity of 70 ± 5% with free access to food and water. All of the experimental procedures were performed in accordance with the principles of care and use of laboratory animals and were approved by the Institutional Animal Care and Use Committee of Xiamen University.

1.20 *In Vivo/Ex Vivo* Fluorescence Imaging. DiR as a hydrophobic and lipophilic near-infrared fluorescence dye was used to label PEG-EPI-PC NPs and MTX-PEG-EPI-PC NPs, respectively (designed as DiR-loaded PEG-EPI-PC NPs and MTX-PEG-EPI-PC NPs, respectively). We used HeLa tumor-bearing BALB/c nude mice as models, developed by subcutaneous injection of HeLa cells. When the tumor diameter was approximately 8 mm, the DiR-loaded PEG-EPI-PC NPs or MTX-PEG-EPI-PC NPs (1 mg/kg) was intravenously injected into HeLa tumor-bearing mice via the tail vein. The time-dependent tumor targeting capacity of DiR-loaded PEG-EPI-PC NPs and MTX-PEG-EPI-PC NPs was imaged at 1, 4, 12, and 24 h post-injection using an IVIS Lumina II imaging system (Caliper Life Sciences, Hopkinton, MA, USA). The mice were sacrificed at 24 h post-injection. The major organs (liver, spleen, kidney, lung, and heart) and tumor were excised and then washed with cold saline for the *ex vivo* fluorescence imaging of DiR fluorescence. All datas were calculated using the region-of-interest (ROS) function of Analysis Workstation software (ART Advanced Research Technologies Inc., Montreal, Canada).

Briefly, the tumor samples were frozen in optimal cutting temperature (O. C. T., Tissue-Tek) embedding medium, cut into 5 mm sections, and stored at -20 °C before use. The frozen tumor sections were fixed in ice-cold acetone for 5 min, air dried for

10 min, and incubated with PBS for 10 min to dissolve the OCT. Then 0.1% triton X-100 was added to permeabilize the cells for 4 min at room temperature. The fluorescence images of the tumor sections were acquired on a Leica TCS SP5 confocal laser scanning microscopy.

1.21 *In Vivo* Anticancer Effect. HeLa tumor bearing BALB/c mice were divided into six groups (five mice per group) in a way to minimize weight and tumor size differences. When the tumor volume reached about 100 mm^3, normal saline (0.9% NaCl), free EPI, free EPI plus free MTX, PEG-EPI-PC NPs, MTX-PEG-EPI-PC NPs (via amide bond) and MTX-PEG-EPI-PC NPs (via imine bond) were intravenously administrated at a EPI-equivalent dose of 5.0 mg/kg and MTX-equivalent dose of 2.4 mg/kg at day 0, 3, and 6. The tumor sizes were measured by a caliper every two days and tumor volumes were calculated as $a \times b^2/2$, in which a and b were respectively the largest and the smallest diameter. The relative tumor volumes were calculated as the current tumor volumes normalized to their initial tumor volume. In addition, the body weights were also measured every two days.

1.22 Histological Analysis. At the 16st day, the mice treated with different formulations were euthanized, and the tumor as well as the main organs were excised, weighed, washed with 0.9% NaCl thrice, and fixed in the 10% neutral buffered formalin. For the hematoxylin and eosin (H&E) staining, the formalin-fixed tumors and main organs were embedded in paraffin blocks, cut into 5 mm sections, stained with H&E, and examined by optical microscope (DM5500B, Leica Microsystems, Germany).

1.23 *In Vivo* Safety. The healthy BALB/c mice were randomly divided into 4 groups: (a) 0.9% NaCl group as the control, (b) PEG-EPI-PC NPs group, (c) MTX-PEG-EPI-PC NPs (via amide bond) group, and (d) MTX-PEG-EPI-PC NPs (via imine bond) group. 200 μL of different formulations were separately injected into mice via the tail vein for four times at interval of three days. At the 16st day, ~0.8 mL of blood was collected from mice to investigate the haematological analyses. The haematological results were measured and compared with the control group.

1.24 Statistical Analysis. All experiments were repeated at least three times. All data were expressed as mean ± standard deviation (SD) value. Statistical tests were performed by the Student's *t*-test and one-way ANOVA. The statistical difference was considered to be significant when the *P* value was less than 0.05.

2. Figures and Captions

Table S1. Average hydrodynamic diameter, PDI, and zeta potential of PEG-EPI-PC NPs, MTX-PEG-EPI-PC NPs, dye-labeled PEG-EPI-PC NPs, and dye-labeled MTX-PEG-EPI-PC NPs.

	Hydrodynamic diameter (D_h, nm)	PDI	Zeta potential (ζ)
PEG-EPI-PC NPs	88.5 ± 5.9	0.126 ± 0.083	-28.3 ± 4.6
MTX-PEG-EPI-PC NPs	92.6 ± 3.8	0.137 ± 0.055	-25.2 ± 2.5
DiD-labeled PEG-EPI-PC NPs	86.2 ± 4.7	0.138 ± 0.042	-28.6 ± 3.9
DiR-labeled PEG-EPI-PC NPs	87.1 ± 2.6	0.121 ± 0.058	-27.5 ± 5.5
DiD-labeled MTX-PEG-EPI-PC NPs	91.7 ± 3.3	0.129 ± 0.035	-25.6 ± 3.7
DiR-labeled MTX-PEG-EPI-PC NPs	90.8 ± 4.2	0.104 ± 0.065	-24.9 ± 2.9
NBD-labeled MTX-PEG-EPI-PC NPs	94.1 ± 5.3	0.167 ± 0.022	-23.7 ± 3.2

Table S2. Average hydrodynamic diameter, PDI, and zeta potential of PEG-EPI-PC NPs and MTX-PEG-EPI-PC NPs.

	MTX-PEG-EPI-PC NPs (via imine bond)	MTX-PEG-EPI-PC NPs (via amide bond)
Hydrodynamic diameter (D_h, nm)	92.6 ± 3.8	90.7 ± 5.3
PDI	0.137 ± 0.055	0.144 ± 0.121
Zeta (ζ) potential (mV)	-25.2 ± 2.5	-24.5 ± 3.7

Dual-drug loading content (%)	22.2 ± 1.5	22.5 ± 1.4
EPI-drug loading content (%)	15.3 ± 0.9	15.5 ± 0.6
MTX-drug loading content (%)	6.9 ± 0.5	7.0 ± 0.7

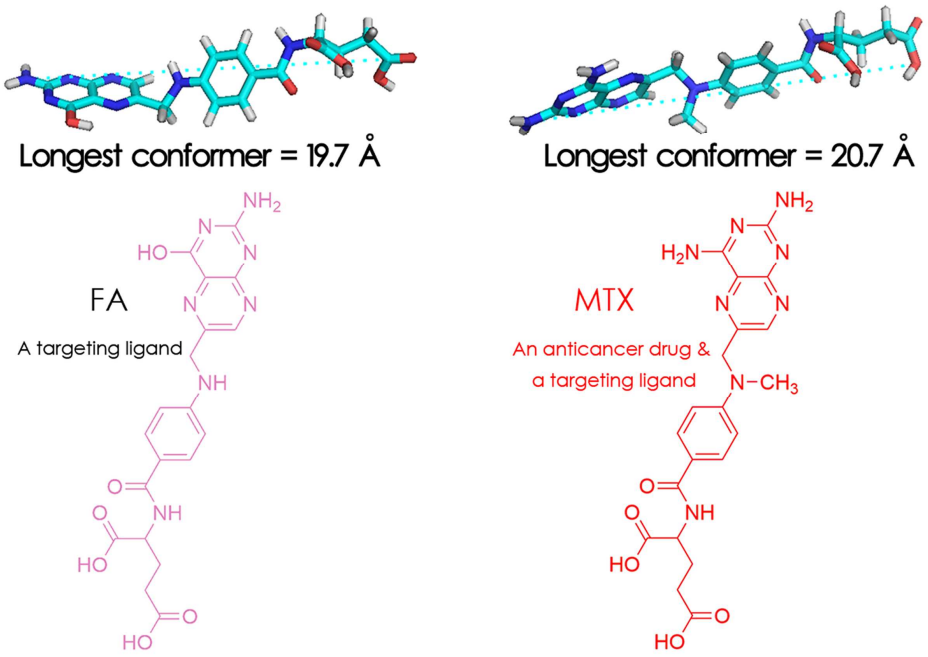

Figure S1. Detailed optimized molecular structures and chemical structures of FA and MTX. MTX is an analogue of FA because of structural similarity, regardless a key feature that MTX has an amino group whereas FA has a hydroxyl group at the 4-position of pteridine ring.

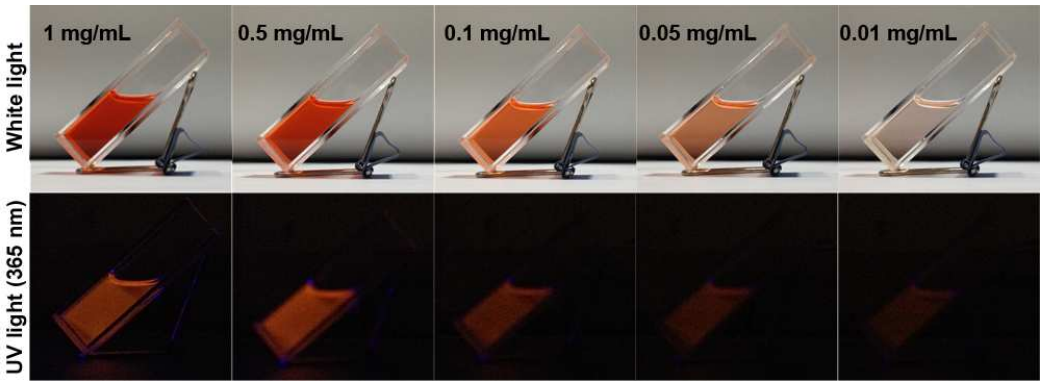

Figure S2. Photographs of EPI-PC complex dispersed in organic phase (DCM) at different concentration under white light or UV light.

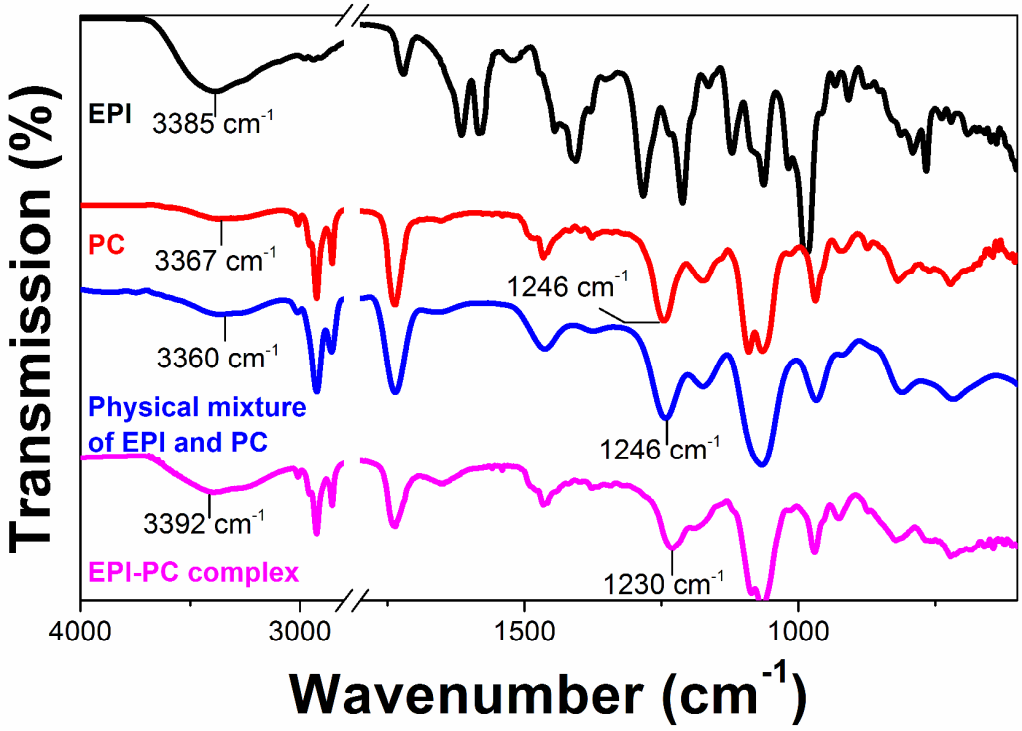

Figure S3. Detailed FT-IR spectra of EPI, PC, physical mixture of EPI and PC, and EPI-PC complex.

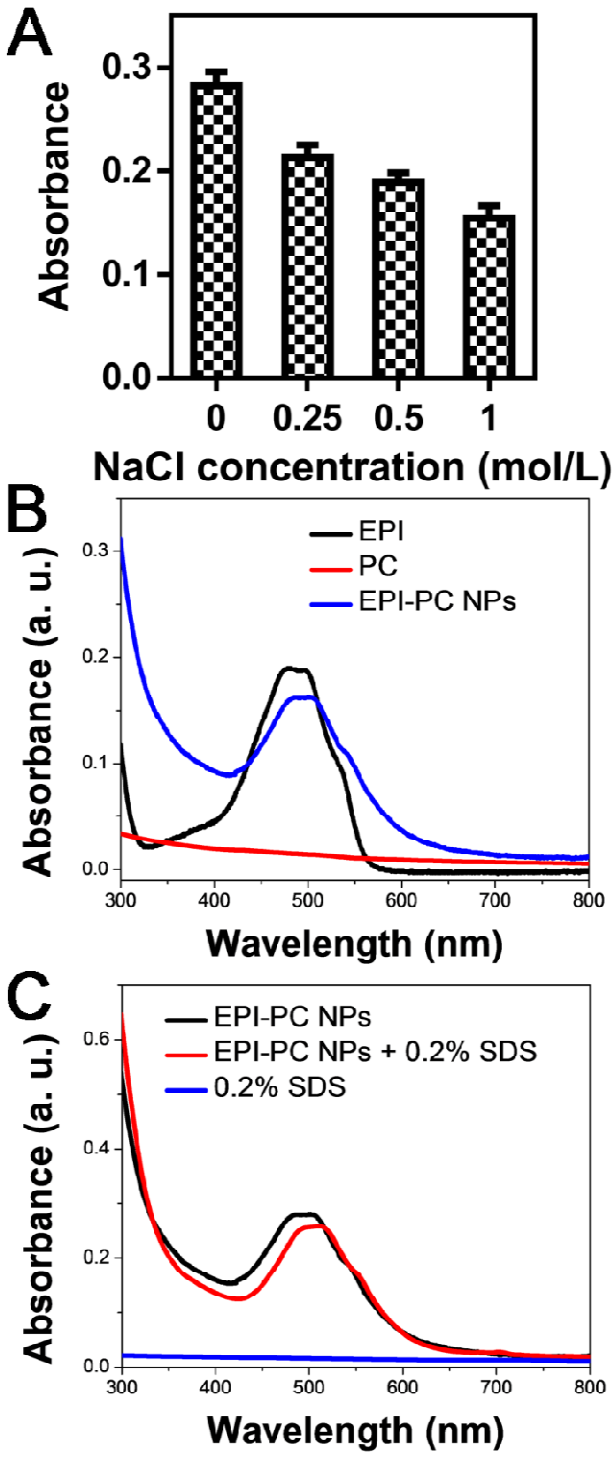

Figure S4. (A) Turbidity changes (absorbance at 488 nm) of EPI-PC NPs (self-assembled by only amphiphilic EPI-PC complex, unPEGyalted EPI-PC NPs) with addition of various amounts of 0.9% NaCl. (B) UV-vis absorption spectra of EPI, PC, and EPI-PC NPs. (C) UV-vis absorption spectra of EPI-PC NPs, free 0.2% SDS (w/v), and EPI-PC NPs with addition of 0.2% SDS. Error bars indicate SD (n = 3).

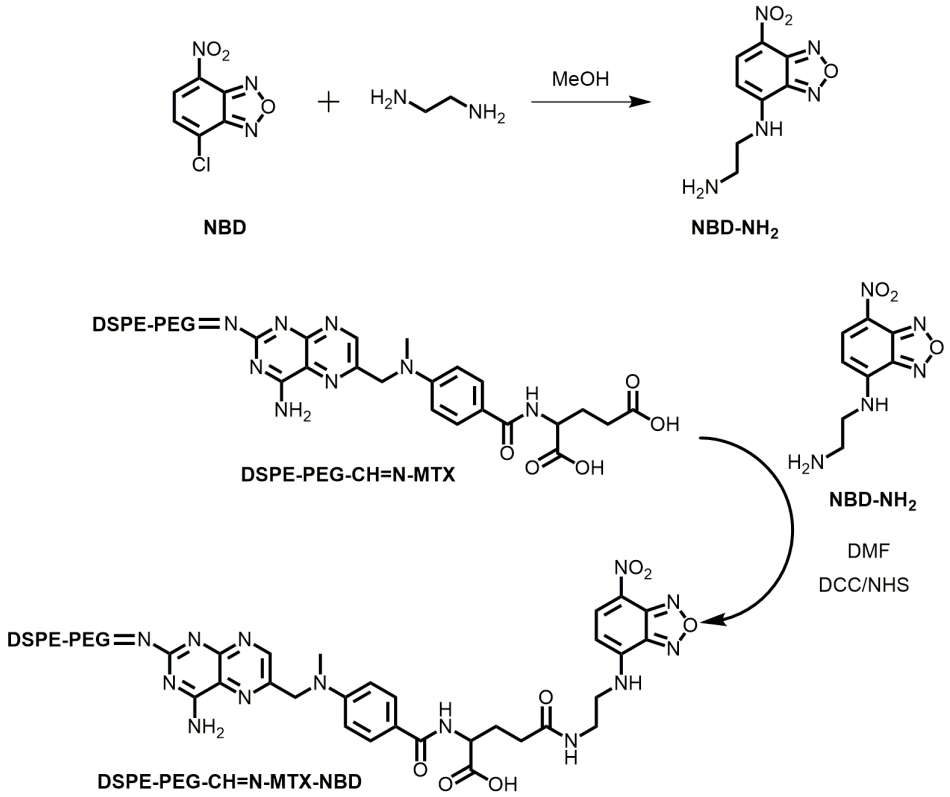

Figure S5. Synthetic route of NBD-labeled DSPE-PEG-CH=N-MTX conjugate. DSPE-PEG-CH=N-MTX-NBD was coupled via amide reaction between amino group of NBD-NH_2 and carboxyl group of MTX moiety.

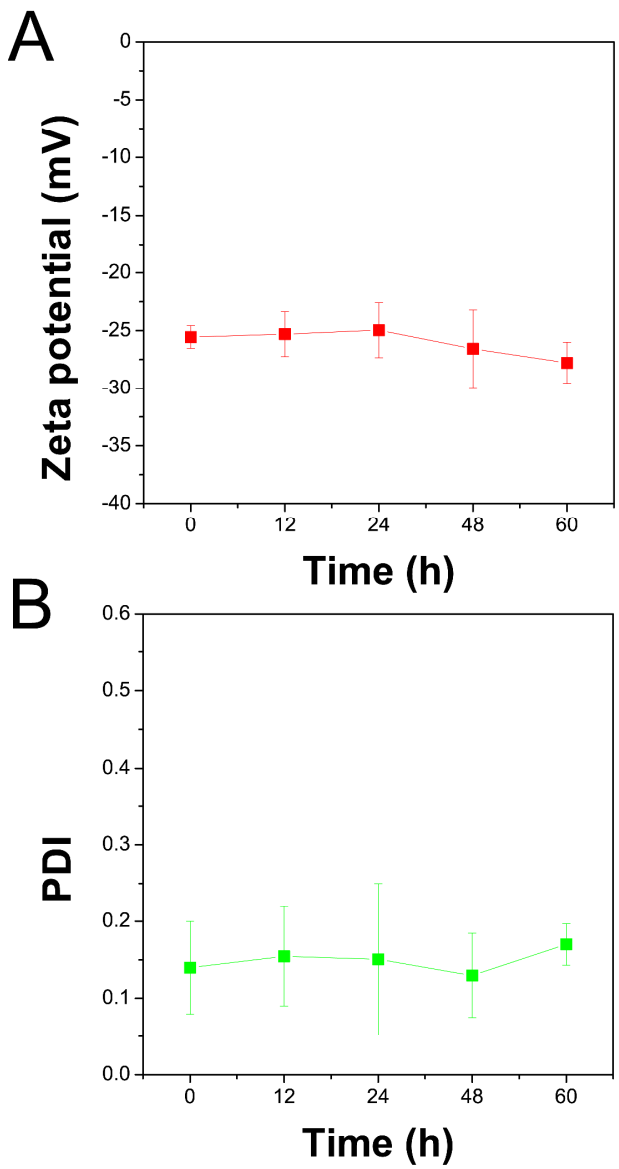

Figure S6. Change of (A) zeta potential and (B) PDI of MTX-PEG-EPI-PC NPs in DI water during storage for 60 h. Error bars indicate SD (n = 3).

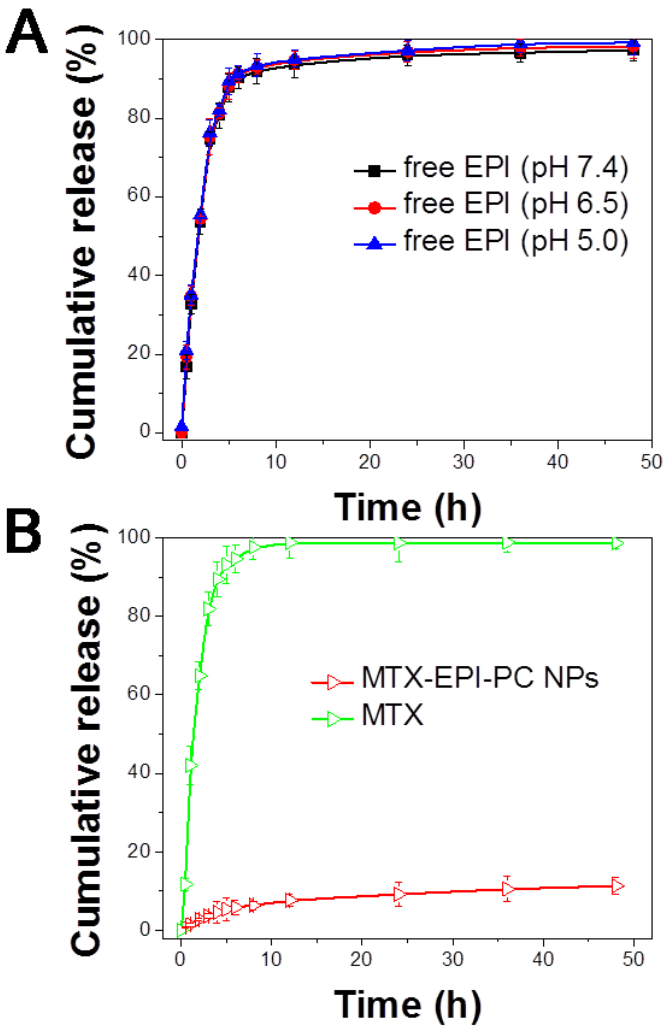

Figure S7. (A) *In vitro* release profiles of EPI from free EPI in buffer (pH 7.4, 6.5, and 5.0) at 37 °C. (B) *In vitro* release profiles of MTX from MTX-PEG-EPI-PC NPs in PBS buffer (pH 7.4) at 37 °C. Error bars indicate SD (n = 3).

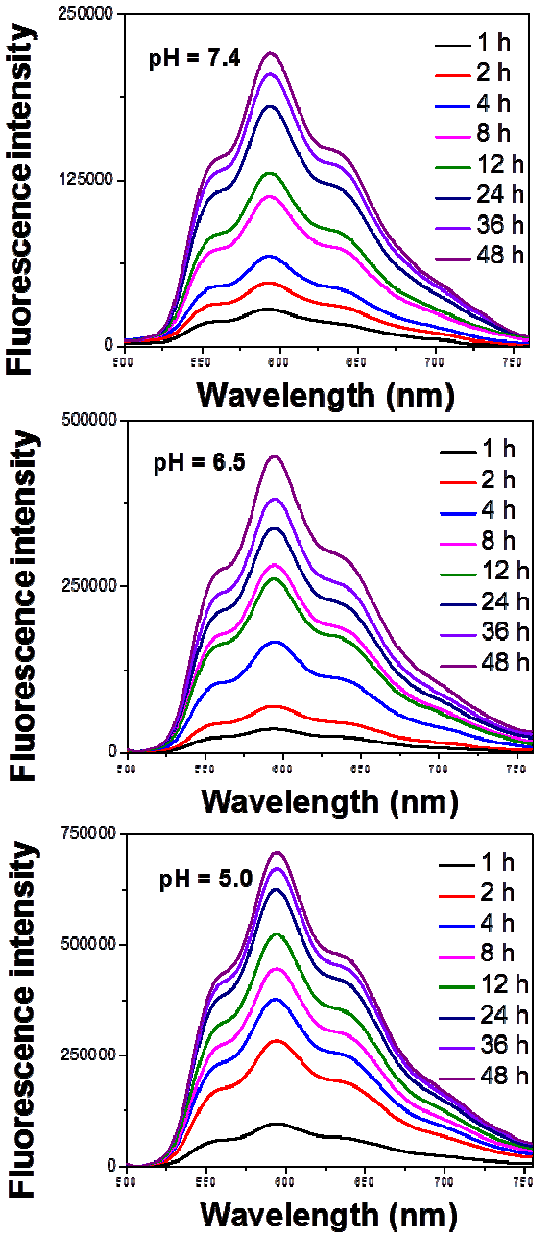

Figure S8. Fluorescence emission spectra of MTX-PEG-EPI-PC NPs in buffer (pH 7.4, 6.5, and 5.0) after kept for 48 h.

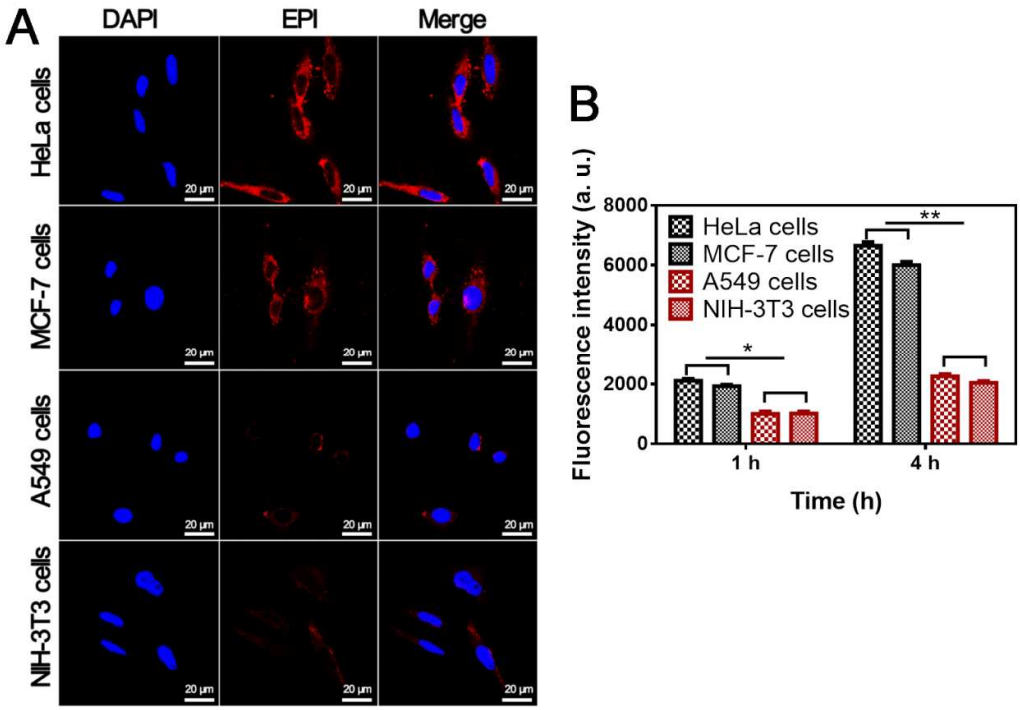

Figure S9. (A) Confocal laser scanning microscopy images and (B) fluorescence intensity determined by flow cytometry of target cells (HeLa and MCF-7 cells with high expression of folate receptors) and non-target cells (A549 and NIH-3T3 cells with low expression of folate receptors) incubated with MTX-PEG-EPI-PC NPs in the absence or presence of free FA for 4 h. Blue represents nuclei stained by DAPI. The scale bar = 20 μm. Error bars indicate SD (n = 3). *P < 0.05.

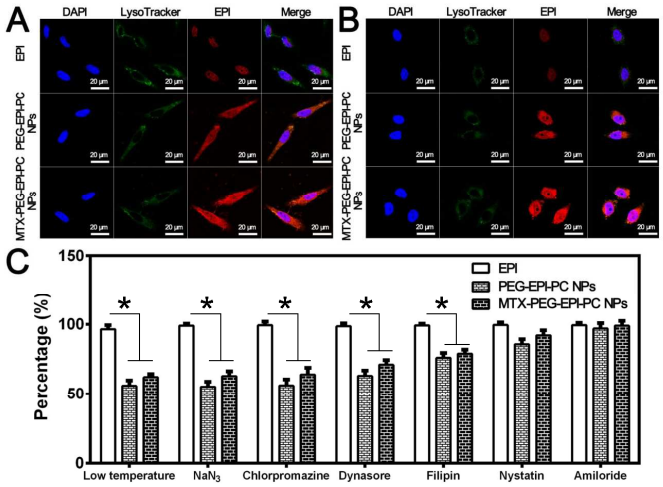

Figure S10. Subcellular localization and endocytosis pathways of MTX-PEG-EPI-PC NPs. (A, B) Subcellular localization of free EPI, PEG-EPI-PC NPs, and MTX-PEG-EPI-PC NPs in (A) HeLa cells or (B) MCF-7 cells after incubation for 4 h. DAPI was used to stain nucleus. Lysotracker Green DND-26 was used to stain endo/lysosomes. The scale bar = 20 μm. (C) Endocytosis inhibition of free EPI, PEG-EPI-PC NPs, and MTX-PEG-EPI-PC NPs in HeLa cells pre-treated with ATP depletion and endocytosis inhibitors. Error bars indicate SD (n = 3). *P < 0.05.

The endocytosis pattern, mechanism, and pathways were investigated by using APT depletion and endocytosis inhibitors including chlorpromazine/dynasore (clathrin-mediated endocytosis inhibitor), filipin (caveolae-mediated endocytosis inhibitor), nystatin (lipid raft-mediated endocytosis inhibitor) and amiloride (macropinocytosis inhibitor). [10] Treatment with chlorpromazine, dynasore, or filipin significantly decreased the cellular uptake of MTX-EPI-PC NPs in HeLa cells (P < 0.05), indicating that both clathrin- and caveolae-mediated endocytosis pathway was involved in the cellular uptake of MTX-EPI-PC NPs by HeLa cells. In addition, treatment with low temperature or NaN_3 induced intracellular ATP depletion and thus markedly decreased the cellular uptake of MTX-EPI-PC NPs, indicating that MTX-EPI-PC NPs entered HeLa cells via an energy-dependent endocytosis process. Taking together, these results above and subcellular localization (see Figure 5) demonstrated that MTX-EPI-PC NPs could be selectively recognized by folate receptors in HeLa cells via multivalent MTX ligand-folate receptor binding interactions and then were energy-dependently internalized into endosomes/lysosomes via a multiple endocytic pathway including both clathrin- and caveolae-mediated endocytosis.

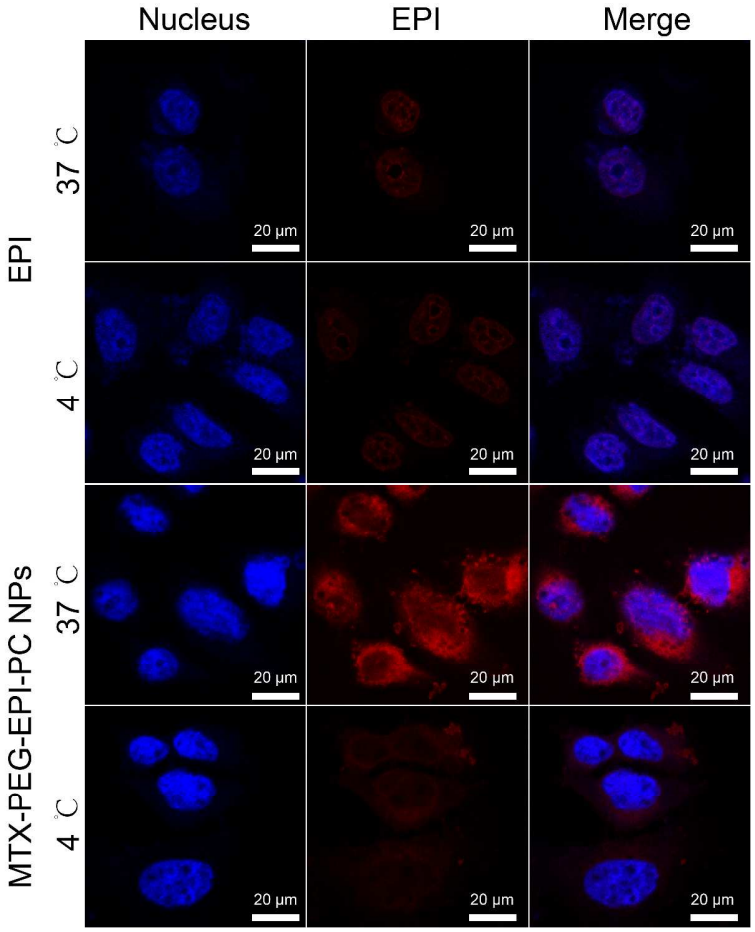

Figure S11 Confocal laser scanning microscopic images of HeLa cells incubated with MTX-PEG-EPI-PC NPs with/without the treatment of low temperature for 1 h. Free EPI was used for comparison.

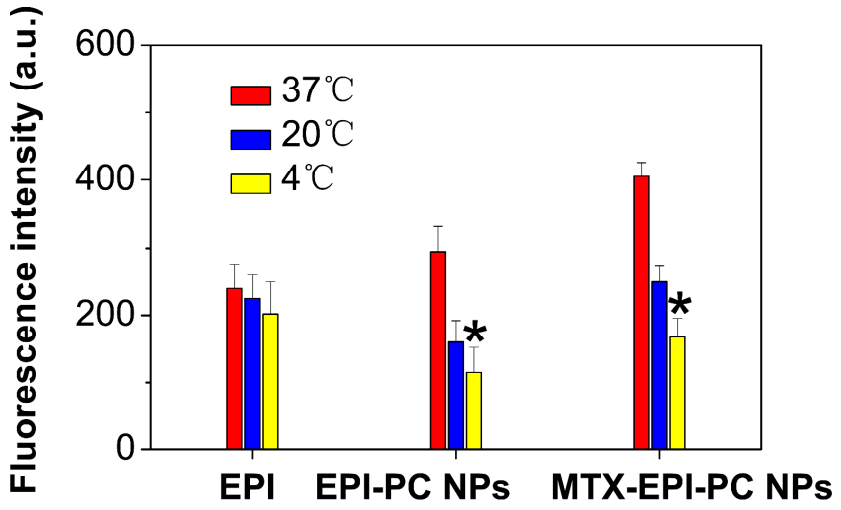

Figure S12. Fluorescence intensity determined by flow cytometry of of HeLa cells treated with free EPI, PEG-EPI-PC NPs, and MTX-PEG-EPI-PC NPs at 37, 20, and 4°C. Error bars indicate SD (n = 3). *P < 0.05.

The fluorescence intensity of MTX-PEG-EPI-PC NPs was much lower in HeLa cells at 4 °C and 20 °C than 37°C. The results indicated that the endocytosis of MTX-PEG-EPI-PC NPs was dependent on both folate receptors (see Figure 4 and 5) and temperature.

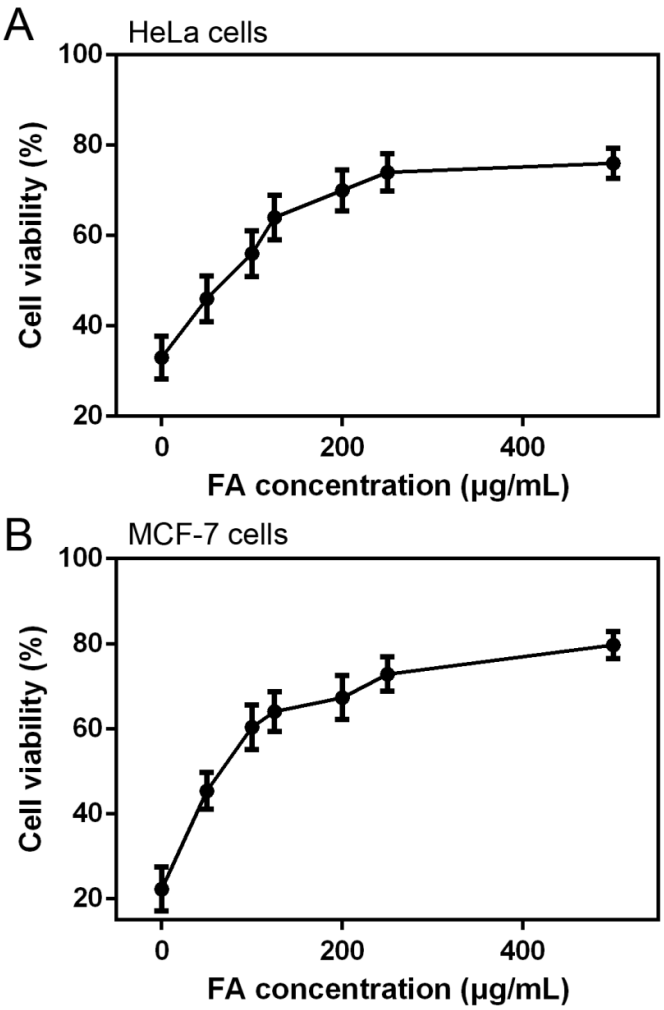

Figure S13. Effect of pretreatment of free FA on cell viability of (A) HeLa or (B) MCF-7 cells incubated with MTX-PEG-EPI-PC NPs at EPI concentration of 5 μg/mL. Error bars indicate SD (n = 3).

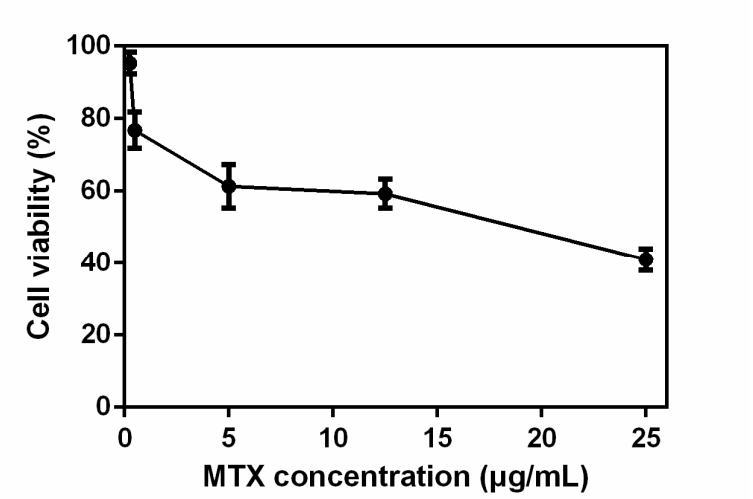

Figure S14. *In vitro* cell viability of HeLa cells treated with free MTX after incubation of 24 h. Error bars indicate SD (n = 4).

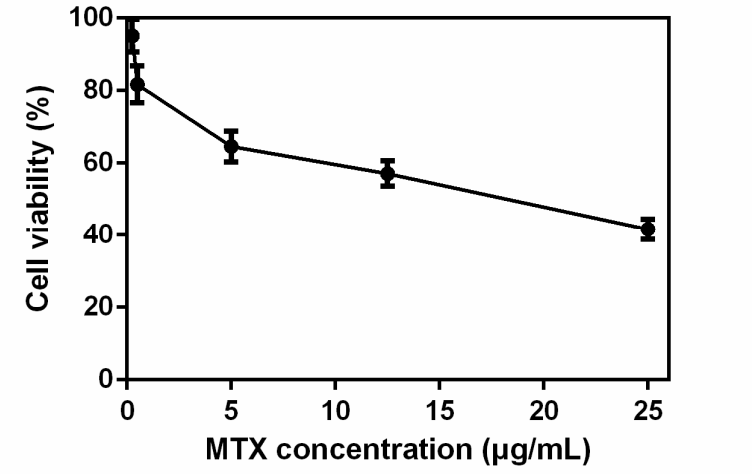

Figure S15. *In vitro* cell viability of MCF-7 cells treated with free MTX after incubation of 24 h. Error bars indicate SD (n = 4).

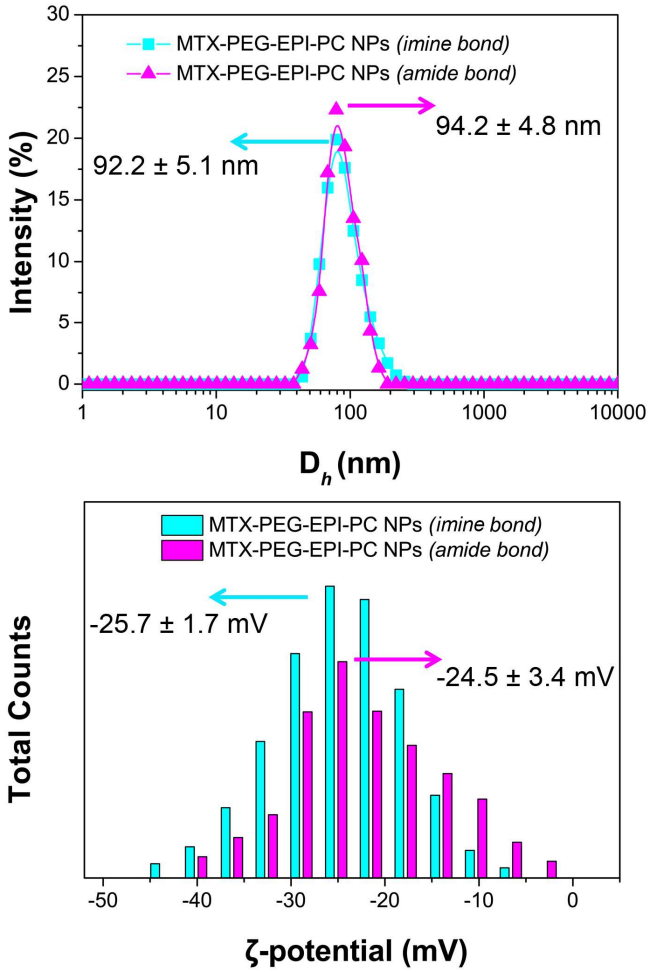

Figure S16. Comprehensive comparison of MTX-PEG-EPI-PC NPs (via imine bond) and MTX-PEG-EPI-PC NPs (via amide bond). (A) hydrodynamic diameter (D_h) and (B) zeta (ζ) potential.

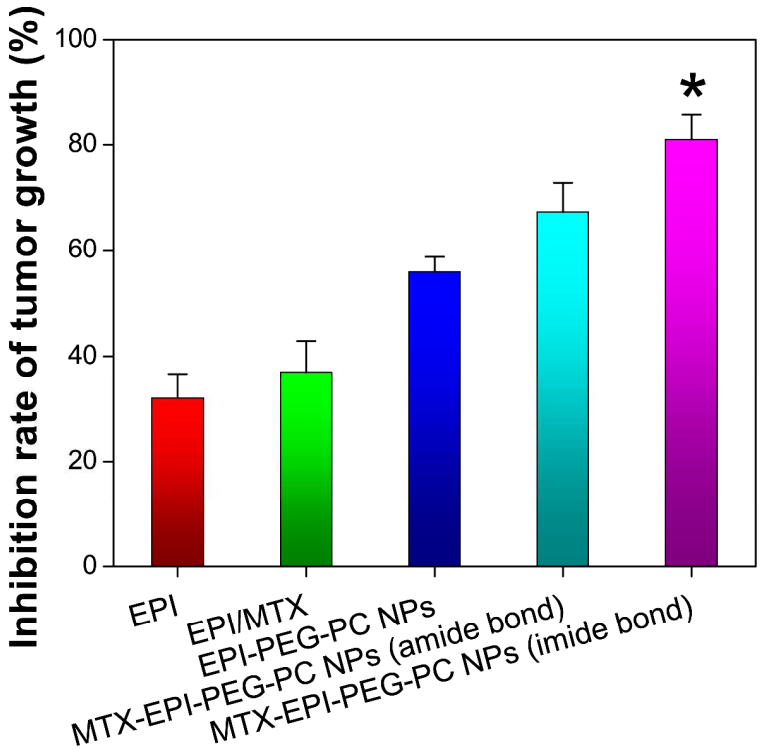

Figure S17. Inhibition rate of tumor growth of HeLa tumor-bearing mice at 24 h post-injection after intravenous injection of free EPI, free EPI plus free MTX, PEG-EPI-PC NPs, and MTX-PEG-EPI-PC NPs (*amide bond*), and MTX-PEG-EPI-PC NPs (*imine bond*). Error bars indicate SD ($n = 5$). *$P < 0.05$.

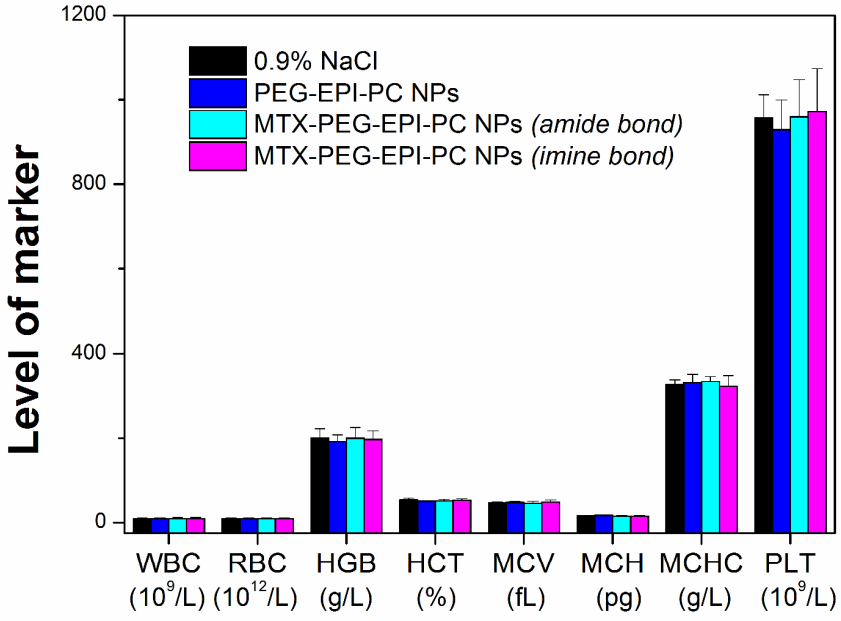

Figure S18. Haematological results of mice treated with different formulations for 16

days. The main parameters are following: white blood cells (WBC), red blood cells (RBC), haemoglobin (HGB), haematocrit (HCT), mean corpuscular volume (MCV), mean corpuscular haemoglobin (MCH), mean corpuscular haemoglobin concentration (MCHC), and platelets (PLT). Error bars indicate SD (n = 6).

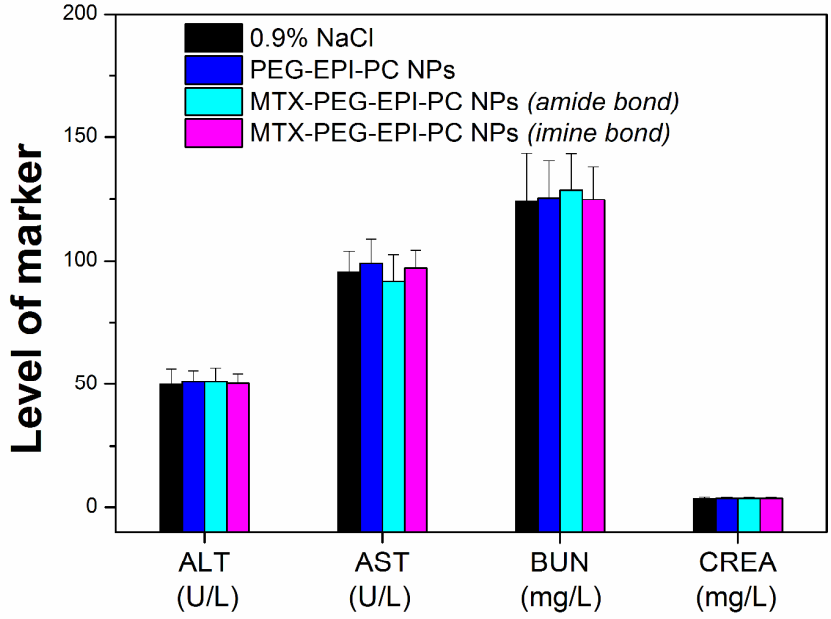

Figure S19. Serological results of mice treated with different formulations for 16 days. The main parameters are following: alanine transaminase (ALT), aspartate transaminase (AST), blood urea nitrogen (BUN), and creatinine (CREA). Error bars indicate SD (n = 6).

References

1. Zalipsky, Samuel; Brandeis, Ester; Newman, Mary S.; Woodle, Martin C. Long Circulating, Cationic Liposomes Containing Amino-Peg-Phosphatidylethanolamine. *FEBS Lett.* **1994,** *353*, 71-74.
2. Zheng, J. N.; Xie, H. G.; Yu, W. T.; Liu, X. D.; Xie, W. Y.; Zhu, J.; Ma, X. J. Chitosan-G-Mpeg-Modified Alginate/Chitosan Hydrogel Microcapsules: A Quantitative Study of the Effect of Polymer Architecture on the Resistance to Protein Adsorption. *Langmuir* **2010,** *26*, 17156-17164.
3. Li, Y.; Lin, J.; Wu, H.; Jia, M.; Yuan, C.; Chang, Y.; Hou, Z.; Dai, L. Novel Methotrexate Prodrug-Targeted Drug Delivery System Based on Peg-Lipid-Pla Hybrid Nanoparticles for Enhanced Anticancer Efficacy and Reduced Toxicity of Mitomycin C. *J. Mater. Chem. B* **2014,** *2*, 6534-6548.
4. Guo, Y.; Zhang, Y.; Ma, J.; Li, Q.; Li, Y.; Zhou, X.; Zhao, D.; Song, H.; Chen, Q.; Zhu, X. Light/Magnetic Hyperthermia Triggered Drug Released from Multi-Functional Thermo-Sensitive Magnetoliposomes for Precise Cancer Synergetic Theranostics. *J. Control. Release* **2017**, doi.org/10.1016/j.jconrel.2017.1004.1028.
5. Li, Y.; Lin, J.; Huang, Y.; Li, Y.; Yang, X.; Wu, H.; Wu, S.; Xie, L.; Dai, L.; Hou, Z. Self-Targeted, Shape-Assisted, and Controlled-Release Self-Delivery Nanodrug for Synergistic Targeting/Anticancer Effect of Cytoplasm and Nucleus of Cancer Cells. *ACS Appl. Mater. Interfaces* **2015,** *7*, 25553-25559.
6. Liu, G.; Ma, J.; Li, Y.; Li, Q.; Tan, C.; Song, H.; Cai, S.; Chen, D.; Hou, Z.; Chen, Q.; Zhu, X. Core-Interlayer-Shell Fe3o4@Msio2@Lipid-Peg-Methotrexate Nanoparticle for Multimodal Imaging

and Multistage Targeted Chemo-Photodynamic Therapy. *Int. J. Pharm.* **2017,** *521*, 19-32.
7. Hou, Z.; Li, Y.; Huang, Y.; Zhou, C.; Lin, J.; Wang, Y.; Cui, F.; Zhou, S.; Jia, M.; Ye, S.; Zhang, Q. Phytosomes Loaded with Mitomycin C-Soybean Phosphatidylcholine Complex Developed for Drug Delivery. *Mol. Pharmaceutics* **2013,** *10*, 90-101.
8. Bao, Y.; Yin, M.; Hu, X.; Zhuang, X.; Sun, Y.; Guo, Y.; Tan, S.; Zhang, Z. A Safe, Simple and Efficient Doxorubicin Prodrug Hybrid Micelle for Overcoming Tumor Multidrug Resistance and Targeting Delivery. *J. Control. Release* **2016,** *235*, 182-194.
9. Li, Y.; Lin, J.; Wu, H.; Chang, Y.; Yuan, C.; Liu, C.; Wang, S.; Hou, Z.; Dai, L. Orthogonally Functionalized Nanoscale Micelles for Active Targeted Codelivery of Methotrexate and Mitomycin C with Synergistic Anticancer Effect. *Mol. Pharmaceutics* **2015,** *12*, 769-782.
10. Wei, T.; Liu, J.; Ma, H.; Cheng, Q.; Huang, Y.; Zhao, J.; Huo, S.; Xue, X.; Liang, Z.; Liang, X. J. Functionalized Nanoscale Micelles Improve Drug Delivery for Cancer Therapy in Vitro and in Vivo. *Nano Lett.* **2013,** *13*, 2528-2534.